

Copyright is owned by the Author of the thesis. Permission is given for a copy to be downloaded by an individual for the purpose of research and private study only. The thesis may not be reproduced elsewhere without the permission of the Author.

**THE SYNTHESIS AND CHARACTERIZATION  
OF NEW HIGHER NUCLEARITY ARENE-  
RUTHENIUM-SULFUR CLUSTERS**

A thesis presented in partial  
fulfillment of the requirements  
for the degree of  
Master of Science  
in Chemistry  
at

Massey University  
New Zealand

Libei Guo  
1999

## ACKNOWLEDGEMENT

I sincerely thank my supervisor Dr. A. H. Wright for his encouragement, guidance and assistance in many ways and for his many hours spent on reading and modifying my thesis. I also thank him for helping me with my papers and many other things in my life. He is not only a very good supervisor in my research work, but also a very good friend of mine.

Thank you very much:

Professor A. M. Brodie and Associate Professor D. R. K. Harding for encouraging me to continue my study and research work.

Dr. A. H. Wright and Dr. A. K. Burrell for their assistance with calculations on quantum study and X ray crystallography.

Dr. P. Edward for his assistance with  $^1\text{H}$  NMR spectrometry.

Members of the Chemistry Department with help and advice; in particular Mr. W. Campbell, Mr. G. H. Freeman and Mr. T. W. G. Canton.

**ABBREVIATION**

cymene	1-isopropyl-4-methylcymene
en	ethylenediamine
NMR	nuclear magnetic resonance
NNEt <sub>2</sub> en	N,N-diethylethylenediamine
DBU	1,8-diazabicyclo[5.4.0]undec-7-ene
IR	infra red
THF	tetrahydrofuran
DMSO	dimethylsulphoxide
TLC	thin layer chromatography
Me	methyl
Cp	cyclopentadiene
Cp'	CH <sub>3</sub> C <sub>5</sub> H <sub>5</sub> (MeCp)
Cp*	Me <sub>5</sub> Cp
Ph	phenyl
Triphos	MeC(CH <sub>2</sub> PPh <sub>2</sub> ) <sub>3</sub>
Cod	cycloocta-1,5-diene
'S <sub>4</sub> '	1,2-bis((2-mercaptophenyl)thiol)ethane(2-)
Cl <sub>4</sub> -cat	tetrachlorocatecholate
<sup>i</sup> Pr	isopropyl

## ABSTRACT

This thesis describes a project investigating the synthesis and characterization of new higher nuclearity arene-ruthenium-sulfur clusters and arene-ruthenium-nitrogen complexes.

The thesis is divided into four chapters, with the introduction in Chapter One. The synthesis and characterization of new higher nuclearity arene-ruthenium-sulfur clusters are described in Chapter Two. These include two novel clusters,  $[\text{Ru}_5\text{S}_4(\text{cymene})_4](\text{PF}_6)_2$ ,  $[\text{Ru}_4(\text{S}_2)(\text{SO})(\text{cymene})_4](\text{PF}_6)_2$  and one known cluster,  $[\text{Ru}_3\text{S}_2(\text{cymene})_3](\text{PF}_6)_2$ . The X-ray crystallographic structures of these three arene-ruthenium-sulfur clusters are discussed in detail including how the number of valence electrons influences the structure, how the solid state structure and single crystal structure effect each other and how the structures determine the chemical shifts and other characters of the clusters. The unusual signals of these three clusters on  $^1\text{H}$  NMR spectra are discussed carefully. The mechanisms of formation of arene-ruthenium-sulfur clusters are described in detail. Some electrochemistry and calculations (quantum chemistry) are also involved.

The synthesis and characterization of arene-ruthenium-nitrogen complexes are described in Chapter Three. These include two new mono-nuclear complexes,  $[\text{RuCl}_2(\text{NH}_3)(\text{cymene})]$ ,  $[\text{Ru}(\text{NH}_3)_3(\text{cymene})](\text{PF}_6)_2$ , one novel amide dimer  $[\text{RuCl}(\text{NH}_2)(\text{cymene})]_2$  and one known complex,  $[\text{RuCl}(\text{NH}_3)_2(\text{cymene})]\text{PF}_6$ . The mechanisms of reactions in which they are formed are also discussed. In Chapter Four, the experimental data is presented.

The X ray crystallography of  $[\text{Ru}_5\text{S}_4(\text{cymene})_4](\text{PF}_6)_2$ ,  $[\text{Ru}_4(\text{S}_2)(\text{SO})(\text{cymene})_4](\text{PF}_6)_2$ ,  $[\text{RuCl}_2(\text{NH}_3)(\text{cymene})]$  and  $[\text{RuCl}(\text{NH}_2)(\text{cymene})]_2$  is described in detail.

# INDEX

Acknowledgements	
Abbreviations	
Abstract	
Index	
List of tables and schemes	
List of figures	

## CHAPTER ONE INTRODUCTION

1.1. Transition metal compounds	1
1.1.1. Transition metal clusters	2
1.1.2. Iron-sulfur clusters and their functions	5
1.1.3. Ruthenium in Haber-Bosch process and hydrodesulfurization (HDS)	7
1.1.4. Arene as ligands in transition metal clusters	8
1.1.5. Sulfur as ligands in transition metal clusters	12
1.2. Transition metal sulfur complexes for catalysis --hydrodesulfurization (HDS)	15
1.2.1. Industry catalysts and mechanisms	16
1.2.2. Catalytic hydrogenation reactions	18
1.2.3. Catalytic hydrogenolysis reactions	19
1.2.4. Catalytic desulfurization reactions	19
1.3. Nitrogenases and dinitrogen reduction	20
1.3.1. Transition metal mono- or bi-nuclear complexes in dinitrogen reduction	23
1.3.2. Transition metal clusters in dinitrogen reduction	24
1.4. Clusters in hydrogenases and hydrogenation	25
1.5. New arene ruthenium sulfur clusters	27

## CHAPTER TWO SYNTHESIS OF ARENE-RUTHENIUM -SULFUR CLUSTERS

2.1. Synthetic strategy	28
2.2. Formation of arene ruthenium sulfur clusters	30
2.2.1. Formation of $[\text{Ru}_3\text{S}_2(\text{cymene})_3](\text{PF}_6)_2$	31
$^1\text{H}$ NMR spectra of $[\text{Ru}_3\text{S}_2(\text{cymene})_3]^{2+}$	31
Electrospray mass spectrum of $[\text{Ru}_3\text{S}_2(\text{cymene})_3](\text{PF}_6)_2$	36
The structure of $[\text{Ru}_3\text{S}_2(\text{cymene})_3](\text{PF}_6)_2$	37
2.2.2. Formation of $[\text{Ru}_5\text{S}_4(\text{cymene})_4](\text{PF}_6)_2$	39
Structure of $[\text{Ru}_5\text{S}_4(\text{cymene})_4](\text{PF}_6)_2$	43
The central ruthenium atom	46
Cymene loss	47
Valence electrons and the structure	48
Dihedral angles	50
Molecular aggregation and molecular structure	53
2.2.3. Formation of $[\text{Ru}_4\text{S}_2(\text{SO})(\text{cymene})_4](\text{PF}_6)_2$	55
The big cluster	56

<sup>1</sup> H NMR spectrum of [Ru <sub>4</sub> (S <sub>2</sub> )(SO)(cymene) <sub>4</sub> ](PF <sub>6</sub> ) <sub>2</sub> cluster	58
The structure of [Ru <sub>4</sub> S <sub>2</sub> (SO)(cymene) <sub>4</sub> ](PF <sub>6</sub> ) <sub>2</sub>	59
Disordered structure	61
Clusters with SO ligands	61
Disulfur as ligand compared to SO	62
Formation of SO ligand in [Ru <sub>4</sub> S <sub>2</sub> SO(cymene) <sub>4</sub> ] <sup>2+</sup> cluster	63
Comparison of chemical shifts of the three clusters	65
The unusual <sup>1</sup> H NMR signals of the cymene-ruthenium-sulfur clusters	66
2.3. Electrochemistry of arene-ruthenium- sulfur clusters	70
2.4. Conditions of the reaction that influence the distribution of the products	74
Temperature	74
pH	75
Amount of NH <sub>4</sub> PF <sub>6</sub>	76
Amount of Na <sub>2</sub> S	76
2.5. Proposed mechanism of formation of the clusters	77
SH <sup>-</sup> and S <sup>2-</sup>	77
[Ru <sub>2</sub> (μ <sub>2</sub> -SH) <sub>2</sub> (cymene) <sub>2</sub> ] and [Ru <sub>2</sub> (μ <sub>2</sub> -S) <sub>2</sub> (cymene) <sub>2</sub> ] fragments	77
Formation of metal-metal bond from the bridged metal atoms	81
Cubane type cluster and coordination	82
Conclusion and future work	83
2.4. Reactions of arene-ruthenium-sulfur clusters	85
With H <sup>+</sup>	85
With H <sub>2</sub>	85
With N <sub>2</sub>	85
<sup>1</sup> H NMR AND MASS SPECTROMETRY DATA FOR CLUSTERS OF	
CHAPTER TWO	87

CHAPTER THREE ARENE-RUTHENIUM-  
NITROGEN COMPLEXES

3.1. Introduction	88
3.2. Synthetic strategy	91
3.3. Formation of cymene-ruthenium-nitrogen complexes	92
3.3.1. Formation of the bis-ammonia complex [RuCl(NH <sub>3</sub> ) <sub>2</sub> (η <sup>6</sup> -cymene)]PF <sub>6</sub>	93
From the dimer [RuCl <sub>2</sub> (η <sup>6</sup> -cymene)] <sub>2</sub>	93
Shielding effect and chemical shift	93
Forming in liquid ammonia	97
From the mono-ammonia complex [RuCl <sub>2</sub> (NH <sub>3</sub> )(η <sup>6</sup> -cymene)]	98
3.3.2. Formation of the mono-ammonia complex [RuCl <sub>2</sub> (NH <sub>3</sub> )(η <sup>6</sup> -cymene)]	98
From the dimer [RuCl <sub>2</sub> (η <sup>6</sup> -cymene)] <sub>2</sub>	98

From the bis-ammonia complex	101
Compare the chemical shifts of these two ammonia complexes	102
The equilibria between the crystals and the solution	102
3.3.3. Formation of the tris-ammonia complex $[\text{Ru}(\text{NH}_3)_3(\eta^6\text{-cymene})](\text{PF}_6)_2$	103
From the dimer $[\text{RuCl}_2(\eta^6\text{-cymene})]_2$	103
From the dimer $[\text{RuCl}_2(\eta^6\text{-cymene})]_2$ with ammonia in methanol	104
Compare the chemical shifts of the three mono-nuclear complexes	106
3.3.4. Formation of the amide dimer $[\text{RuCl}(\text{NH}_2)(\eta^6\text{-cymene})]_2$	107
From the bis-ammonia complex $[\text{RuCl}(\text{NH}_3)_2(\eta^6\text{-cymene})]\text{PF}_6$	107
Chemical shifts of three dimeric complexes	110
3.3.5. Discussion of the reaction conditions	111
Temperature	111
Amount of base	111
Solvent	112
Inert atmosphere	112
Conclusions	112
3.4. Reactions of cymene-ruthenium-nitrogen complexes	113
3.4.1. Reactions of the bis-ammonia complex	113
With DBU	113
With triethylamine	113
With $\text{AgNO}_3$ and Zn	114
3.4.2. Reactions of the mono-ammonia complex $[\text{RuCl}_2(\text{NH}_3)(\eta^6\text{-cymene})]$	114
With $\text{AgNO}_3$	115
With sodium anthracene	115
3.4.3. Reactions of the tris-ammonia complex $[\text{Ru}(\text{NH}_3)_3(\eta^6\text{-cymene})](\text{PF}_6)_2$	115
3.4.4. Reactions of the amide dimer $[\text{RuCl}(\text{NH}_2)(\eta^6\text{-cymene})]_2$	117
With $[\text{Ru}(\text{acetone})_3(\eta^6\text{-cymene})]^{2+}$	117
With $[\text{Ru}(\text{acetonitrile})_3(\eta^6\text{-cymene})](\text{NO}_3)_2$	117
Thermolysis of the amide dimer	118
Reaction with DBU	118
With acid $\text{CF}_3\text{COOH}$	119
3.5. Conclusions and further research	120
$^1\text{H}$ NMR, IR AND MASS SPECTROMETRY DATA FOR THE COMPOUNDS OF CHAPTER THREE	122

#### CHAPTER FOUR EXPERIMENTAL

4.1. General	123
material	123
method	123
4.2. Preparation of arene-ruthenium-sulfur clusters	123
$[\text{Ru}_3\text{S}_2(\text{cymene})_3](\text{PF}_6)_2$	124
$[\text{Ru}_5\text{S}_4(\text{cymene})_4](\text{PF}_6)_2$	124
$[\text{Ru}_4\text{S}_2(\text{SO})(\text{cymene})_4](\text{PF}_6)_2$	124
Reactions of arene-ruthenium-sulfur clusters with $\text{H}_2$ and $\text{N}_2$	125



4.3. Preparation of arene-ruthenium-nitrogen complexes	125
4.3.1. Preparation of $[\text{RuCl}(\text{NH}_3)_2(\eta^6\text{-cymene})]\text{PF}_6$	125
4.3.2. Preparation of $[\text{RuCl}_2(\text{NH}_3)(\eta^6\text{-cymene})]$	125
4.3.3. Preparation of $[\text{Ru}(\text{NH}_3)_3(\eta^6\text{-cymene})](\text{PF}_6)_2$	126
4.3.4. Preparation of $[\text{RuCl}(\text{NH}_2)(\eta^6\text{-cymene})]_2$	126
4.5. Reactions of $[\text{RuCl}(\text{NH}_2)(\eta^6\text{-cymene})]_2$	127
With $[\text{Ru}(\text{acetone})_3(\text{cymene})]^{2+}$	127
With $[\text{Ru}(\text{acetonitrile})_3(\text{cymene})]^{2+}$	127
Reaction with DBU	127

REFERENCES	128
------------	-----

## LIST OF TABLES AND SCHEMES

Table 1	Chemical shifts, Ru-N bondlengths and distances of cymene-Ru for two cationic complexes with nitrogen containing ligands	97
Table 2	Crystallographic data of the mono-ammonia complex	101
Table 3	Chemical shifts, bond lengths of Ru-N and distances of Ru-cymene for the two ammonia complexes	102
Table 4	Product distribution influenced by pH	75
Table 5	Chemical shifts of three mono-nuclear ammonia complexes	106
Table 6	Selected X ray crystallographic data of $[\text{Ru}_5\text{S}_4(\text{cymene})_4](\text{PF}_6)_2$	46
Table 7	Calculated charges of the central Ru atom and side Ru atoms	47
Table 8	Selected data of $[\text{Ru}_4(\text{S}_2)(\text{SO})(\text{cymene})_4]^{2+}$ X ray structure	60
Table 9	Chemical shifts, bond lengths of Ru-N and the distances of Ru-cymene for three dimeric complexes	110
Table 10	data of X ray crystallography of $[\text{RuCl}(\text{NH}_2)(\eta^6\text{-cymene})]_2$	107
Table 11	Data of X-ray crystallography of $[\text{Ru}_3\text{S}_2(\text{cymene})_3](\text{PF}_6)_2$	38
Table 12	Bond lengths vary with their valence electron numbers of some bowtie clusters	50
Table 13	Dihedral angles of some bowtie clusters	51
Scheme 1	Structure change from $[\text{Ru}_3\text{S}_2(\text{cymene})_3]^{2+}$ to $[\text{Ru}_3\text{S}_2(\text{cymene})_3]^0$	4
Scheme 2	Localization-delocalization patterns of iron sulfur clusters	6
Scheme 3	Ways arene rings coordinate to metal atoms	8
Scheme 4	The principal mechanism for heterogeneous HDS of thiophene	17
Scheme 5	The proposed mechanism of hydrogenation using $[\text{Rh}(\text{cod})(\text{PPh}_3)_2]^+$	18
Scheme 6	Desulfurization of thiophenes by $[\text{Ru}_3(\text{CO})_{12}]$	20
Scheme 7	Activation of dinitrogen by sulfur bridge with hydrogen on it	22
Scheme 8	Tetranuclear intermediate of dinitrogen binding on $[\text{V}_3(\text{catcholte})_3]$	25
Scheme 9	Redox equilibrium catalyzed by hydrogenases	26
Scheme 10	The proposed mechanism of heterolytic cleavage of dihydrogen	26
Scheme 11	Dihydrogen cleaved at Ru-S sites of cluster $[\text{Ru}(\text{PCy}_3)(\text{S}_4)]$	26
Scheme 12	Proton transfer from metal-SH complexes to coordinated dinitrogen	14
Scheme 13	The reaction scheme of cymene-ruthenium-nitrogen complexes	120
Scheme 14	Sulfur atom removed by $[(\text{Cp}')_2\text{Mo}_2\text{Co}_2\text{S}_3(\text{CO})_4]$	17
Scheme 15	Reaction scheme of bis-ammonia complex	92
Scheme 16	Disordered structure of $[\text{Ru}_4\text{S}_2(\text{SO})(\text{cymene})_4](\text{PF}_6)_2$	61
Scheme 17	$[\text{Cp}^*\text{RuCl}(\mu_2\text{-SH})_2]$ as precursors and difference between Rh, Ir compounds and Ru compound	80
Scheme 18	Formation mechanism of arene-ruthenium-sulfur clusters	84
Scheme 19	$\eta^6$ -to- $\eta^4$ change of the arene ring	9
Scheme 20	Interior magnetic field and donor/acceptor characters of the cymene ring	96
Scheme 21	Dihydrogen absorption of $[\text{Ru}_4(\text{benzene})_4\text{H}_4]^{2+}$	88

## LIST OF FIGURES

Figure 1	Structure of cubane cluster $[\text{Fe}_4\text{S}_4]$	2
Figure 2	Structures of $[(\text{benzene})_4\text{Ru}_4(\text{OH})]^{4+}$ and a stereo ligand (S)-(-)BINAP	4
Figure 3	Structures of sulfite reductase and carbon monoxide Dehydrogenase	5
Figure 4	Structures of $[\text{Ru}_4\text{H}_4(\text{benzene})_4]^{2+}$ and $[\text{Ru}_3\text{S}_2(\text{cymene})_3]^{2+}$	12
Figure 5	Structures of $(\text{Et}_4\text{N})_2[(\text{Cl}_4\text{-cat})(\text{CH}_3\text{CN})\text{MoFe}_3\text{S}_4\text{Cl}_3]$ and $[\text{Ru}_4\text{S}_4\text{Cp}^*_4]^{2+}$	15
Figure 6	Structure of nitrogenase clusters	21
Figure 7	$^1\text{H}$ NMR spectrum of $[\text{Ru}_3\text{S}_2(\text{cymene})_3]^{2+}$ in $\text{CDCl}_3$	34
Figure 8	$^1\text{H}$ NMR spectrum of $[\text{Ru}_3\text{S}_2(\text{cymene})_3]^{2+}$ in $\text{D}_6\text{-acetone}$	35
Figure 9	$^1\text{H}$ NMR spectrum of $[\text{Ru}_3\text{S}_2(\text{cymene})_3]^{2+}$ in $\text{CD}_2\text{Cl}_2$	35
Figure 10	Electrospray mass spectrum of $[\text{Ru}_3\text{S}_2(\text{cymene})_3](\text{PF}_6)_2$	37
Figure 11	Structure of $[\text{Ru}_3\text{S}_2(\text{cymene})_3]^0$	39
Figure 12	$^1\text{H}$ NMR spectrum of $[\text{Ru}_5\text{S}_4(\text{cymene})_4]^{2+}$ in $\text{CDCl}_3$	40
Figure 13	$^1\text{H}$ NMR spectrum of $[\text{Ru}_5\text{S}_4(\text{cymene})_4]^{2+}$ in $\text{D}_6\text{-acetone}$	41
Figure 14	$^1\text{H}$ NMR spectrum of $[\text{Ru}_5\text{S}_4(\text{cymene})_4]^{2+}$ in $\text{CD}_2\text{Cl}_2$	41
Figure 15a	FAB mass spectrum of $[\text{Ru}_5\text{S}_4(\text{cymene})_4](\text{PF}_6)_2$	42
Figure 15b	Isotopic distribution of FAB mass spectrum of $[\text{Ru}_5\text{S}_4(\text{cymene})_4](\text{PF}_6)_2$	43
Figure 16	ORTEP view of structure of $[\text{Ru}_5\text{S}_4(\text{cymene})_4](\text{PF}_6)_2$	44
Figure 17	Compare the dihedral angle of $[\text{Ir}_4\text{S}_4(\text{Cp}^*)_4\text{Co}]^{2+}$ , $[(\text{Cp}^*\text{Ir})_4\text{S}_4\text{Fe}]^{2+}$ , $[(\text{Cp}^*\text{Ir})_4\text{S}_4\text{Fe}]^+$ and $[\text{Ru}_5\text{S}_4(\text{cymene})_4]^{2+}$	51
Figure 18	Solid state structure of $[\text{Ru}_5\text{S}_4(\text{cymene})_4]^{2+}$	54
Figure 19	$^1\text{H}$ NMR spectrum of the big cluster	57
Figure 20	Electrospray mass spectrum of the big cluster	57
Figure 21	$^1\text{H}$ NMR spectrum of $[\text{Ru}_4(\text{S}_2)(\text{SO})(\text{cymene})_4]^{2+}$	58
Figure 22	ORTEP view of the structure of $[\text{Ru}_4(\text{S}_2)(\text{SO})(\text{cymene})_4](\text{PF}_6)_2$	59
Figure 23	X ray structures of SO containing clusters	62
Figure 24	Cyclic voltammetry of $[\text{Ru}_3\text{S}_2(\text{cymene})_3]^{2+}$	72
Figure 25	Cyclic voltammetry of $[\text{Ru}_4(\text{S}_2)(\text{SO})(\text{cymene})_4]^{2+}$	74
Figure 26	Cyclic voltammetry of $[\text{Ru}_4\text{S}_2(\text{SO})(\text{cymene})_4]^{2+}$	74
Figure 27	$^1\text{H}$ NMR spectrum of the reaction mixture in basic condition	76
Figure 28	$^1\text{H}$ NMR spectrum of $[\text{Ru}_5\text{S}_4(\text{cymene})_4]^{2+}$ with hydrogen	86
Figure 29	Metal-metal bond / nonbond equilibrium of the Ru dimer	82
Figure 30	Metal-metal bond / nonbond equilibrium of Ru-S cubane cluster	82
Figure 31	MO diagram and frontier orbitals of SO	64
Figure 32	IR spectrum of $[\text{RuCl}(\text{NH}_3)_2(\eta^6\text{-cymene})]\text{PF}_6$	94
Figure 33	NMR spectrum of $[\text{RuCl}(\text{NH}_3)_2(\eta^6\text{-cymene})]\text{PF}_6$	94
Figure 34	X ray crystallographic structure of $[\text{RuCl}(\text{NH}_2)(\eta^6\text{-cymene})]_2$	109

Figure 35	IR spectrum of $[\text{RuCl}_2(\text{NH}_3)(\eta^6\text{-cymene})]$	99
Figure 36	NMR spectrum of $[\text{RuCl}_2(\text{NH}_3)(\eta^6\text{-cymene})]$	99
Figure 37	X ray crystallographic structure of $[\text{RuCl}_2(\text{NH}_3)(\eta^6\text{-cymene})]$	100
Figure 38	IR spectrum of $[\text{Ru}(\text{NH}_3)_3(\eta^6\text{-cymene})](\text{PF}_6)_2$	105
Figure 39	NMR spectrum of $[\text{Ru}(\text{NH}_3)_3(\eta^6\text{-cymene})](\text{PF}_6)_2$	105
Figure 40	IR spectrum of $[\text{RuCl}(\text{NH}_2)(\eta^6\text{-cymene})]_2$	108
Figure 41	NMR spectrum of $[\text{RuCl}(\text{NH}_2)(\eta^6\text{-cymene})]_2$	108
Figure 42	Cyclic voltammetry for a reversible reaction	71
Figure 43	From reversibility to irreversibility when sweep rates increase	71
Figure 44	Model of dinitrogen binding to $\text{Fe}_4$ face of Fe/Mo cluster	13
Figure 45	The catalytic cycle for the reduction of $\text{N}_2$ by Mo-nitrogenase of <i>K. pneumoniae</i>	89
Figure 46	NMR spectrum for the reaction of $[\text{Ru}(\text{NH}_3)_3(\eta^6\text{-cymene})](\text{PF}_6)_2$ with two equivalents of DBU	116
Figure 47	NMR spectrum for the reaction of $[\text{Ru}(\text{NH}_3)_3(\eta^6\text{-cymene})](\text{PF}_6)_2$ with four equivalents of DBU	116
Figure 48	NMR for the reaction of $[\text{RuCl}(\text{NH}_2)(\eta^6\text{-cymene})]_2$ with DBU	119
Figure 49	Structures of $80e^-$ and $81e^-$ clusters with nonbonding distances	49
Figure 50	HOMO of $[\text{Ru}_4\text{S}_2(\text{SO})(\text{cymene})_4]^{2+}$ with disulfur and SO ligands	63
Figure 51	Alternative structure of $[\text{Ru}_3\text{S}_2(\text{cymene})_3]^0$	9
Figure 52	Dihedral angle dependence of the total energies for three bowtie clusters	52
Figure 53	Molecular aggregation of $\text{Ru}_6\text{C}(\text{CO})_{11}(\mu_3\text{-}\eta^2\text{:}\eta^2\text{:}\eta^2\text{-C}_6\text{H}_6)(\eta^6\text{-C}_6\text{H}_6)$ and $\text{Ru}_6\text{C}(\text{CO})_{11}(\eta^6\text{-C}_6\text{H}_6)_2$	10
Figure 54	The two pairs of chemically equivalent hydrogen atoms on the cymene ring	32
Figure 55	Different coordination directions of the cymene rings in $[\text{Ru}_4(\text{S}_2)(\text{SO})(\text{cymene})_4](\text{PF}_6)_2$	68
Figure 56	Space filling models of $[\text{Ru}_4(\text{S}_2)(\text{SO})(\text{cymene})_4](\text{PF}_6)_2$ and $[\text{Ru}_5\text{S}_4(\text{cymene})_4](\text{PF}_6)_2$	67
Figure 57	Cymene rings coordinate to Ru atoms in different directions	69
Figure 58	Examples of ruthenium (and osmium) nitrido carbonyl clusters	90
Figure 59	Structures of $[\text{Ti}(\mu_3\text{-N})(\text{Cp}^*)]_4$ and $[\text{V}(\mu_3\text{-N})(\text{Cp}^*)]_4$	91
Figure 60	X ray crystallographic structure of $[\text{Ru}_5\text{S}_4(\text{cymene})_4](\text{PF}_6)_2$	46

# CHAPTER ONE INTRODUCTION

## 1.1. Transition metal compounds

This thesis is about the synthesis and characterization of high nuclearity ruthenium clusters. The underlying motivations for examining these clusters include:

The first involves industrial catalysis and the multi-electron redox reactions such as Haber-Bosch process (nitrogen reduction) and fuel processing (hydrodesulfurization, dehydration and hydrocracking).

Catalysts lie at the heart of many industrial processes. The more efficient the catalysts used, the more energy can be saved in the processes of production. A major task of industrial chemistry is to discover new efficient catalysts. Transition metals and their clusters are one of the main choices for catalysts in industries.

The second involves modeling catalysis either in industrial or biological systems such as nitrogen reduction, hydrogenation and other reductions of small molecules.

Insights into the mechanisms of catalytic processes offer the prospect of improved efficiency. In multi- component heterogeneous sulfide catalysts, many phases are present and more than one active site or reaction channel may be present, and it is not always clear which phase catalyses a given channel.

The chemistry of transition metal clusters has helped the study of heterogeneous catalysts and catalysis in several ways: modes of ligands binding to multi-metallic sites are often the same on metal surfaces and clusters. Ligand transformations on clusters may be used as guides to similar reaction pathways on the heterogeneous catalysts. Clusters may be adsorbed on surfaces and their surface reactions may then be followed by various spectroscopic techniques. The surface structure formed in these reactions are often catalytically active and comparison of the activity of catalysts prepared from organometallic cluster precursors with that of conventionally prepared catalysts can give useful information on active site structures and reaction mechanisms.

In biochemical systems, the exact mechanisms of nitrogenases and hydrogenases are still not yet clear after almost one century of study. Many scientists have tried to mimic and model these processes using synthesized transition metal clusters in vitro, and a lot of progress has been made particularly during the last forty years. It both benefits the mechanisms that are studied in biological and chemical systems at the same time.

### 1.1.1. Transition metal clusters

Transition metal clusters are complexes that contain a group of transition metal atoms joined by metal-metal bonds. A cluster usually contains a metal core surrounded by ligands.

Sometimes, this definition is not very strict. Compounds without metal-metal bonds but with metals joined together by ligands as bridges are also called clusters. For example, iron-sulfur cubane cluster,  $[\text{Fe}_4\text{S}_4]$  is the basic component of many metalloproteins, in which iron atoms are joined together by sulfur atoms as bridges. (Figure 1)

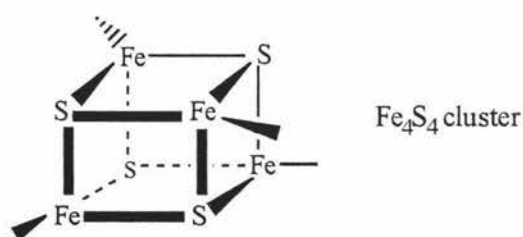


Figure 1 Structure of cubane cluster  $[\text{Fe}_4\text{S}_4]$

There are several aspects that effect the characters of the cluster:

- The type of the metal atoms

Ruthenium and iron are both group eight transition metals, and it is well known that ruthenium has a greater catalytic ability than iron. For example, ruthenium has been

known to be 45 times as catalytically active as its equivalent weight of iron as promoters in Haber-Bosch process <sup>1</sup>.

New complexes of lanthanide and actinide series are providing new insights. Early in 1992, Evans et al. found that a mononuclear  $\eta^2$ -hydrazine samarium complex could be synthesized by protonation of an  $[\text{N}_2\text{H}_2]^{2-}$  complex, which is an interesting models for the mechanism of dinitrogen reduction <sup>2</sup>.

- The number of the metal atoms

The number of the metal atoms in the cluster may influence the ability of the electron storing and transferring, and hence the ability of catalysis. Poly-nuclear clusters usually have more ability of catalysis than corresponding mono- or bi-nuclear complexes. For example, in a recent quantum chemical study, Siegbahn et.al suggested that  $\text{N}_2$  is four-coordinated in the  $[\text{Fe}_8\text{S}_9]^{2-}$  cluster rather than two-coordinated in the dimer model. Add two hydrogen atoms on the bridging sulfur between the cubanes, making all iron atoms  $\text{Fe}^{2+}$ , opens up the cavity for easy access of  $\text{N}_2$ . Hence  $\text{N}_2$  is activated with N-N distance of 1.21 Å in the cluster model rather than 1.19 Å in the dimer model <sup>3</sup>, which indicates that  $\text{N}_2$  is more activated in the cluster model.

- The way that metal atoms joined together

It is different in characters of metal-metal multiple bonds compared to metal-metal single bonds. For example,  $[\text{Os}_3(\text{CO})_{12}]$  is more stable comparing to its unsaturated derivative  $[\text{H}_2\text{Os}_3(\text{CO})_{10}]$  that contains one  $\text{Os}=\text{Os}$  double bond in it <sup>97</sup>.

- The type of the ligands and the mode of coordination

Complexes with sulfur-containing ligands have different properties to those with other element containing ligands, such as oxygen and nitrogen. For example,  $[(\text{benzene})_4\text{Ru}_4(\text{OH})_4]^{4+}$  (Figure 2a) decomposes with hydroxide ion to corresponding bi-nuclear complexes <sup>4</sup>, while  $[(\text{p-cymene})_3\text{Ru}_3\text{S}_2]^{2+}$  just opens one of its metal-metal bond when it gains two electrons giving  $[(\text{p-cymene})_3\text{Ru}_3\text{S}_2]$  (Scheme 1) <sup>5</sup>.

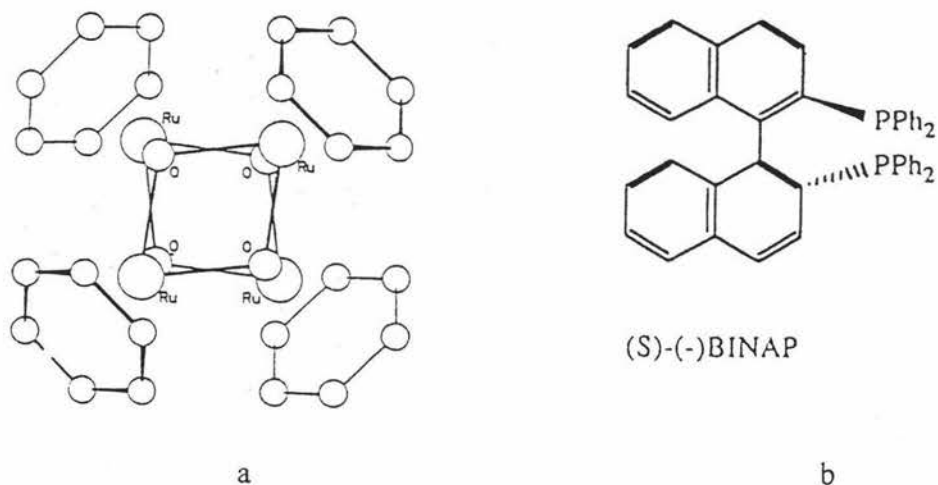
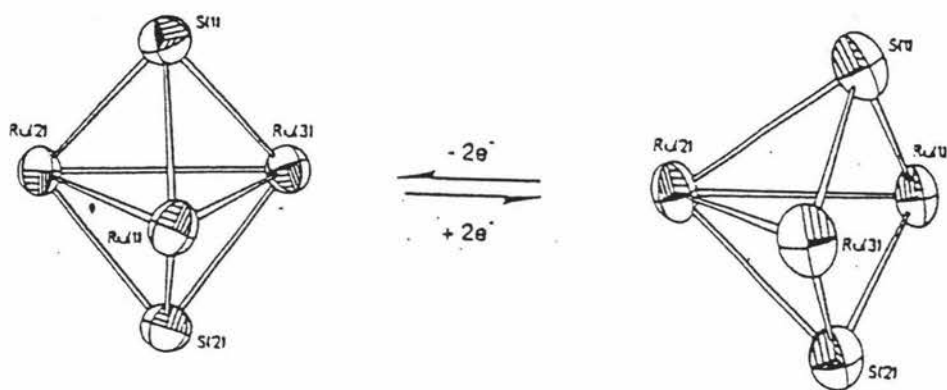


Figure 2. Structures of  $[(\text{benzene})_4\text{Ru}_4(\text{OH})]^{4+}$  and a stereo ligand (S)-(-)-BINAP



Scheme 1 Structure change from  $[\text{Ru}_3\text{S}_2(\text{cymene})_3]^{2+}$  to  $[\text{Ru}_3\text{S}_2(\text{cymene})_3]$

Some complexes have been known with stereo-ligands, which have been designed for special use of catalysts. For example, BINAP-Ru(2+)<sup>6</sup> that produced by treatment of  $[\text{RuCl}_2(\eta^6\text{-benzene})]_2$  with (R)- or (S)-BINAP (Figure 2b) can catalyze the highly enantioselective hydrogenation of functionalized ketones<sup>6</sup> and  $\beta$ -substituted (E)- $\beta$ -(acylamino)acrylic acid<sup>7</sup>.

This project has been targeted at the synthesis and characterization of ruthenium sulfur (also some nitrogen) arene clusters with the underlying aim of modeling catalysis and testing for catalytic activity.



## 1.1.2. Iron-sulfur clusters and their functions

The well known iron sulfur clusters can offer insights that are helpful to design the aim compounds, and one possible role for ruthenium sulfur clusters might be to model the mechanism of iron clusters in biological systems, *vis versa*.

Models that uncover the mechanistic detail of nitrogen reduction are an attractive target. For example,  $[\text{Fe}_4\text{S}_4]$  cluster is the subunit of all the clusters in the three kinds of nitrogenases. There are also three kinds of hydrogenases and except “iron, nickel free” one,  $[\text{Fe}_4\text{S}_4]$  cluster consists the clusters in the other two kinds of hydrogenases. In sulfite reductase, the  $[\text{Fe}_4\text{S}_4]$  cluster is bridged by a cystine sulfur atom to a heme group <sup>8</sup> (Figure 3 a). In the two distinct clusters of carbon monoxide dehydrogenase, it is bridged by an unknown atom to a nickel center cluster <sup>9</sup> (Figure 3 b).

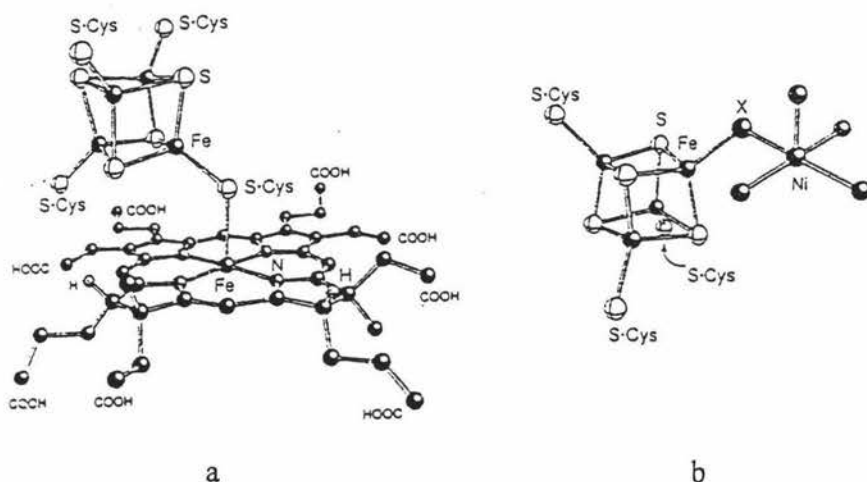
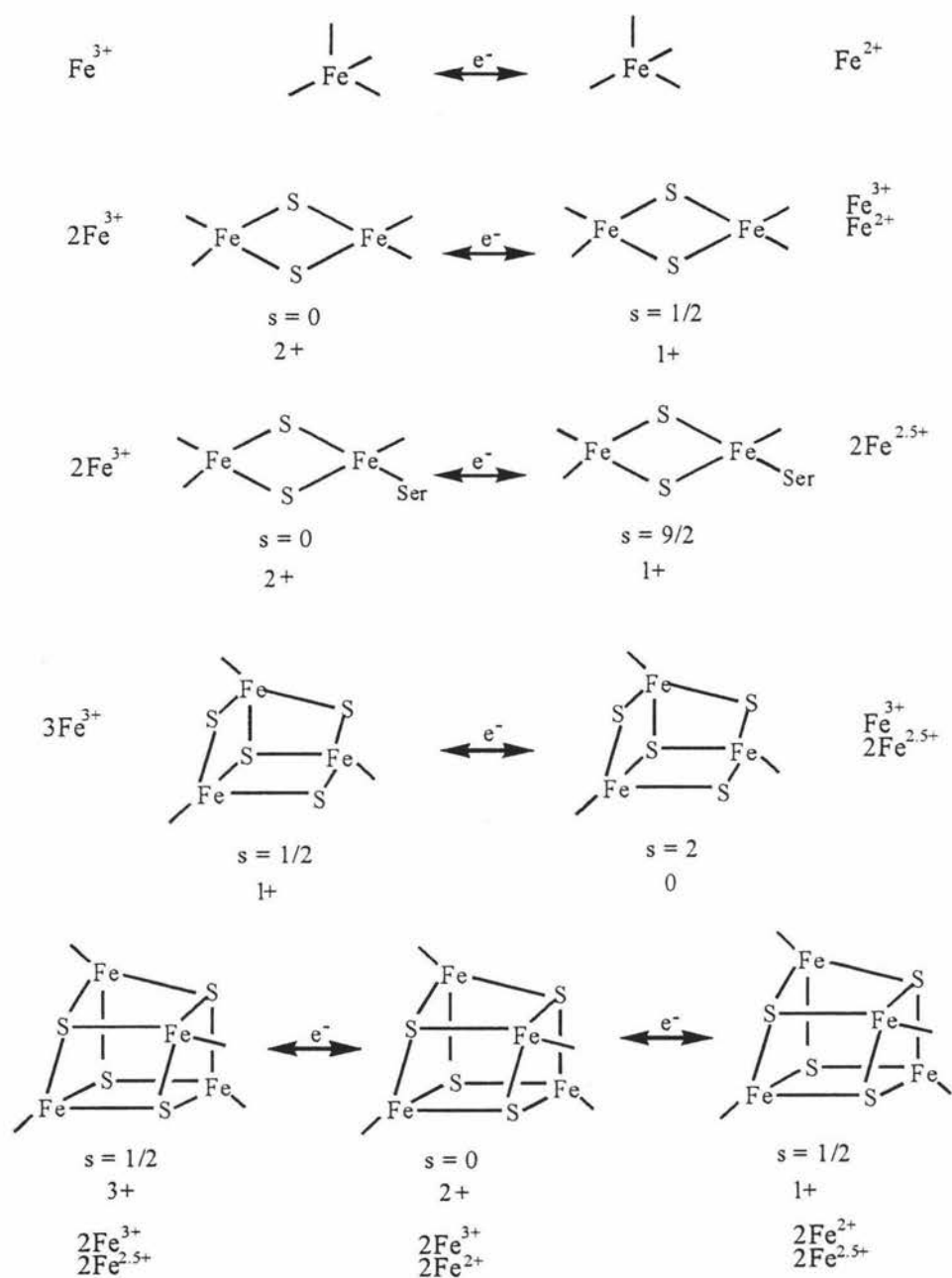


Figure 3 Structures of sulfite reductase and carbon monoxide dehydrogenase

Nature’s modular iron-sulfur clusters include  $[\text{Fe}_2\text{S}_2]$ ,  $[\text{Fe}_3\text{S}_4]$ , and  $[\text{Fe}_4\text{S}_4]$  clusters (scheme 2). There are several ways of showing their structural versatility and robustness. They have facility for conversion and interconversion in both the free and protein bound conditions (chemical systems and biological systems, respectively). They also undergo ligand exchange reactions and oxidative degradation <sup>10</sup>.



Scheme 2 Localization-delocalization patterns of iron sulfur clusters

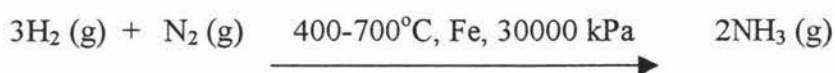
Iron-sulfur clusters have functions of electron transferring, accepting, donating, shifting and storing because of their versatility and robustness. Other functions not of a redox nature have also been discovered. These include the binding and activation of

substrates at the unique iron site of  $[\text{Fe}_4\text{S}_4]$  cluster in the catalytic function of actonitase<sup>11</sup> and related enzymes, and apparently stabilizing radicals in reductions occurring by a free-radical pathway. There is evidence that the clusters can function in coupling electron transfer to proton transport<sup>12</sup>.

Scheme 2 illustrates the localization-delocalization patterns of iron sulfur clusters.  $[\text{Fe}_4\text{S}_4]$  clusters contain delocalized  $\text{Fe}^{2.5+}\text{Fe}^{2.5+}$  pairs in their most common oxidation states<sup>13</sup>. For  $[\text{Fe}_2\text{S}_2]^{1+}$ , only when Cys is mutated to a Ser, the cluster is valence-delocalized with  $S = 9/2$ <sup>14</sup>. The  $[\text{Fe}_3\text{S}_4]^0$  clusters provide strong evidence that the delocalized pair has spin  $S = 9/2$ <sup>15</sup>. Spin-state variability depending on cluster environment is considered as a possible control factor for substrate specificity and gated electron transfer<sup>10</sup>.

### 1.1.3. Ruthenium, Haber-Bosch process and hydrodesulfurization (HDS)

The first Haber-Bosch production plant started up at BASF in 1913<sup>5</sup>. Haber-Bosch process is still the best industrial process for reduction of  $\text{N}_2$  with  $\text{H}_2$  to form ammonia:



The reaction has been running under conditions of high temperature and high pressure. The most widely used catalyst of this process is BASF-developed catalyst that consists of  $\alpha$ -iron as the promoter<sup>16</sup>.

Great energy savings could be obtained by an improvement in catalytic activity of catalysts allowing for operation at lower temperatures and pressures. Therefore, new efficient catalysts that can be used at much milder conditions need to be found.

Ruthenium is considered to possess great potential in development of new catalysts for the ammonia synthesis. In the early 1970s, Ozaki and co-workers introduced

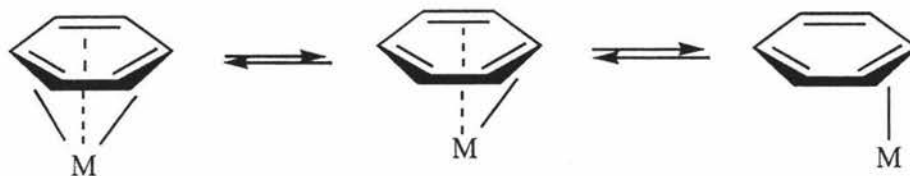
a carbon-supported ruthenium catalyst promoted by alkali metal <sup>17,18</sup> at 250°C and 80 kPa. Ru/AC-K (AC = activated carbon) exhibited a 10-fold increase in the rate of NH<sub>3</sub> synthesis compared to a conventional promoted iron catalyst under similar conditions. Since then, Ru/AC-K has been developed for industrial use <sup>19</sup>. Recently, a number of papers have reported the adsorption and the activation of dinitrogen and dihydrogen on ruthenium catalysts by Izumi et.al <sup>20,21,22</sup>.

Besides this, it is also found that ruthenium has significant ability of catalysis in other processes such as hydrodesulfurization (HDS) process <sup>23,24</sup>. For both heterogeneous and homogeneous catalysts in this process, ruthenium is almost the most active promoters compared to other metals that have been known <sup>25</sup>. (This will be discussed later in section 1.2).

1997-1998, the world production of ammonia is almost 200 million tons, which is still far less than required <sup>26</sup>.

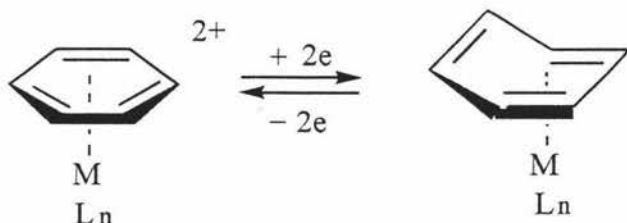
#### 1.1.4 Arene as ligands in transition metal clusters

There are several ways in which arene rings coordinate to metal atoms, such as  $\eta^2$ -,  $\eta^2$ -, and  $\eta^6$ -  $\pi$  coordination <sup>27</sup>, which implies that clusters with arene rings as ligands have great flexibility and robustness, and therefore, the great ability of electron storing and transferring during catalysis processes. (Scheme 3)



Scheme 3 Ways that arene rings coordinate to metal atoms

Geiger <sup>101</sup>, Finke <sup>102</sup> and their co-workers have demonstrated that some cationic metal arene complexes can undergo simultaneous  $2e^-$  reduction. These reductions are associated with a  $\eta^6$ -to- $\eta^4$  change in the hapticity of the arene (Scheme 19).



Scheme 19  $\eta^6$ -to- $\eta^4$  change of the arene ring

Depending on this, Rauchfuss et.al <sup>5</sup> suggest an alternative structural possibility for the  $50e^-$  cluster  $[\text{Ru}_3\text{S}_2(\text{cymene})_3]$ . In this alternative structure the closo  $\text{Ru}_3\text{S}_2$  core is retained, but one arene adopts the  $\eta^4$ - geometry (Figure 51) rather than the  $\eta^6$ - geometry with one metal-metal bond opened. (The open structure was shown in Figure 11.)

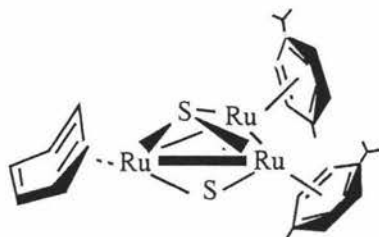


Figure 51 Alternative structure of  $[\text{Ru}_3\text{S}_2(\text{cymene})_3]$

It has also been reported the electrophilic properties of arene rings. Mononuclear systems have been studied quite extensively <sup>107</sup>. For instance the  $[\text{Cr}(\text{CO})_3]$  fragment shows an electron withdrawing effect on coordinating arene rings, resulting in an activation towards the addition of nucleophiles <sup>108</sup>. The influence of a metal cluster should be even larger. Both  $\eta^6$  (terminal) and  $\mu_3\text{-}\eta^2\text{:}\eta^2\text{:}\eta^2$  (face bridging) coordination modes of

the arene rings have been found in many clusters such as  $\text{Os}_3(\text{CO})_9(\mu_3\text{-}\eta^2\text{:}\eta^2\text{:}\eta^2\text{-C}_6\text{H}_6)^{109}$ ,  $\text{Ru}_6\text{C}(\text{CO})_{11}(\mu_3\text{-}\eta^2\text{:}\eta^2\text{:}\eta^2\text{-C}_6\text{H}_6)(\eta^6\text{-C}_6\text{H}_6)^{109}$  and  $\text{Ru}_6\text{C}(\text{CO})_{11}(\eta^6\text{-C}_6\text{H}_6)_2^{110}$ . Different coordination mode leads to different activation of arene rings. When coordinated to a triosmium carbonyl cluster  $\text{Os}_3(\text{CO})_9(\mu_3\text{-}\eta^2\text{:}\eta^2\text{:}\eta^2\text{-C}_6\text{H}_6)$  in the face-capping mode, benzene is activated towards nucleophiles such as  $\text{H}^-$ ,  $\text{Me}^-$  or  $\text{Ph}^-$ , which add the ring in the exo position <sup>111</sup>. In contrast, nucleophiles do not appear to add to plain arenes which are coordinated to a tris-(cyclopentadienylcobalt) cluster <sup>112</sup>.

Different coordination modes of arene rings also lead to different molecular aggregations. For example, it has been found that there are two different kinds of coordination modes of the arene rings in a pair of isomeric bis-arene clusters  $\text{Ru}_6\text{C}(\text{CO})_{11}(\mu_3\text{-}\eta^2\text{:}\eta^2\text{:}\eta^2\text{-C}_6\text{H}_6)(\eta^6\text{-C}_6\text{H}_6)^{109}$  and  $\text{Ru}_6\text{C}(\text{CO})_{11}(\eta^6\text{-C}_6\text{H}_6)_2^{110}$ . In both crystals the benzene ligands face each other in graphitic arrangements, causing the formation of molecular "snakes" and "rows", respectively. (Figure 53) <sup>106</sup>.

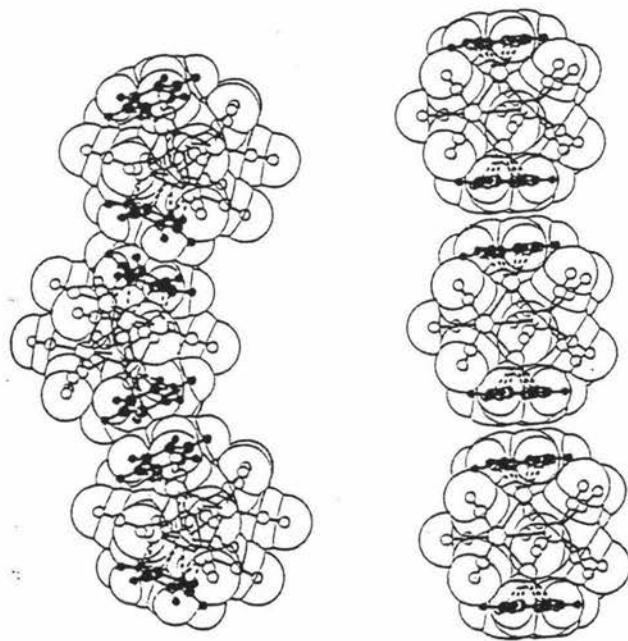


Figure 53 Molecular aggregation of  $\text{Ru}_6\text{C}(\text{CO})_{11}(\mu_3\text{-}\eta^2\text{:}\eta^2\text{:}\eta^2\text{-C}_6\text{H}_6)(\eta^6\text{-C}_6\text{H}_6)$  and  $\text{Ru}_6\text{C}(\text{CO})_{11}(\eta^6\text{-C}_6\text{H}_6)_2$

Central of the arene ruthenium chemistry is the dimeric complex  $[(\text{arene})\text{RuCl}_2]_2$  prepared from the reaction of cyclohexadienes and hydrated ruthenium trichloride<sup>28</sup>. The p-cymene derivative of these dimers was selected for this study because of its good solubility compared to the benzene and hexamethylbenzene derivatives, ease of synthesis from commercially available  $\alpha$ -phellandrene and convenient  $^1\text{H}$  NMR characteristics of its derivatives. The chemical shift of hydrogen atoms on the cymene ring, the methyl group and isopropyl group are all easy to recognize, especially the chemical shift of the four hydrogen atoms on the cymene ring are very specific when the ring coordinates to metal atoms. But the chemical shift of hydrogen atoms on the benzene ring is only one single peak, which is more difficult to identify compared to the cymene ring.

Although the work on ruthenium arene clusters has been done for several decades, very few ruthenium arene clusters have been found. In 1975, Stephenson described the characterization of cubane cluster  $[\text{Ru}_4(\text{OH})_4(\text{benzene})]^{4+}$  (Figure 2 a) formed by the base hydrolysis of  $[(\text{benzene})\text{RuCl}_2]_2$ <sup>29</sup>. The electron-deficient clusters  $[\text{M}_4\text{H}_4(\text{arene})_4]^{2+}$  (M = Ru, Os) has been briefly reported in 1986 (Figure 4 a)<sup>30</sup>, and their properties of activating dihydrogen have been discovered by Suss-Fink et al. in 1993<sup>31</sup>. The first arene ruthenium sulfur cluster  $[(\text{p-cymene})_3\text{Ru}_3\text{S}_2]^{2+}$  (Figure 4 b) was made by Lockmayer et.al using  $[(\text{p-cymene})\text{RuCl}_2]_2$  as starting material in 1989<sup>5</sup>. (This will be discussed in detail later in section 2.2.1.)



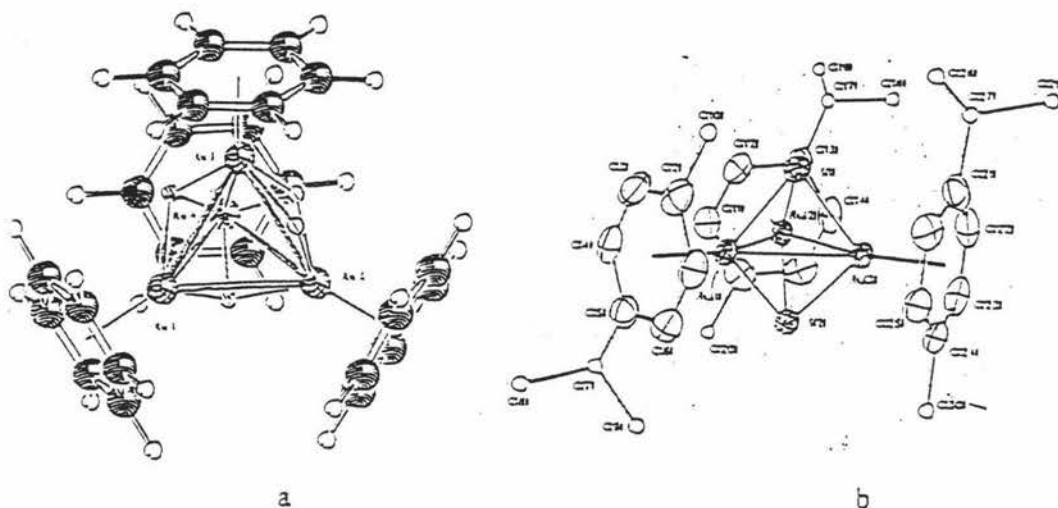
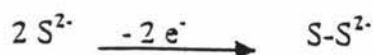


Figure 4 Structures of  $[\text{Ru}_4\text{H}_4(\text{benzene})_4]^{2+}$  and  $[\text{Ru}_3\text{S}_2(\text{cymene})_3]^{2+}$

### 1.1.5. Sulfur as ligands in transition metal clusters

Sulfur-containing compounds have long been known to act as poisons for noble metal catalysts because of their strong coordinating and adsorptive properties, which cause them to block reactive metal sites<sup>32</sup>. Nevertheless, many transition metal sulfides ( $\text{S}^{2-}$ ) display intriguing catalytic activity in their own way. Sulfide ligands form relatively strong bonds with many transition metals, and the ligands can play an important role in stabilizing di- and poly-nuclear complexes against fragmentation process during catalysis<sup>33</sup>. This gives the cluster a metal core that can catalytically store and transfer electrons and protons to molecules.

Sulfur donor ligands tend to favor lower oxidation states of metal ions. The relatively positive reduction potentials of the sulfide complexes, for example, when compared to relative oxygen or nitrogen donor systems, provide a favorable environment for many catalytic reduction reactions that have been characterized<sup>34</sup>. The redox changes of the sulfide complexes can be attributed by changes in the formal oxidation states of the metal ions. However, the ability of coordinated sulfide ligands to participate in redox chemistry, for example,

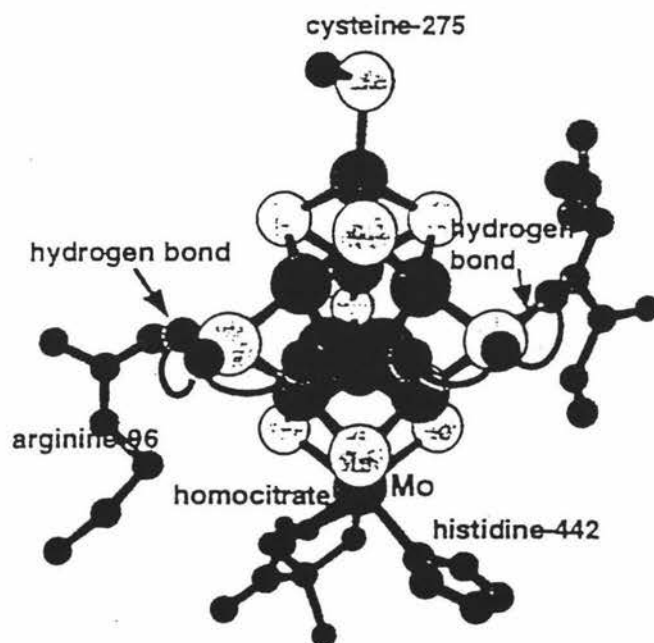




has also been proved <sup>35</sup>.

It has been found that sulfur can act in an important role in the hydrodesulfurization processes. Dihydrogen is split by metal-sulfur center to metal-hydride and thiol hydride <sup>36</sup>.

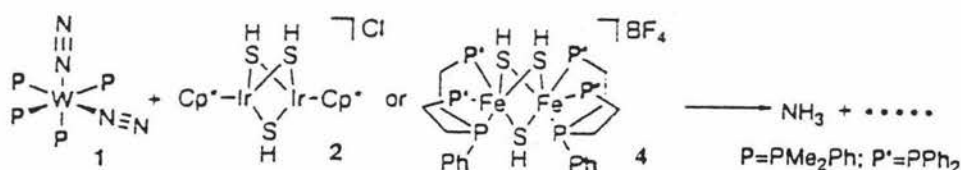
It is claimed that protonation of the activated dinitrogen proceeds with the aid of the bridging hydrosulfido ligands in the Fe/Mo cluster by several groups recently <sup>37</sup>. Dance gave a model of that the bridging sulfido ligands mediate proton transfer to the coordinated dinitrogen bound to the Fe<sub>4</sub> face of the Fe/Mo sulfido cluster via  $\mu$ -SH intermediate (Figure 44) <sup>37c-f</sup>.



The Fe<sub>7</sub>MoS<sub>9</sub>(cysteine)(histidine)(homocitrate) cluster, showing hydrogen bonds from behind the S<sup>2-</sup> atoms flanking the front face, and the postulated transfer of H to bound N<sub>2</sub> by inversion of (S<sup>2-</sup>-H)

Figure 44 Model of dinitrogen binding to Fe<sub>4</sub> face of Fe/Mo cluster

Recently, Hidai et al. have proved this experimentally by investigating the reactivity of dinuclear complexes (Ru, Ir or Rh) containing bridging hydrosulfido ligands toward coordinated dinitrogen on tungsten giving  $\text{NH}_3$ <sup>38</sup>. They have given the first example of proton transfer from metal  $\mu\text{-SH}$  complexes to coordinated dinitrogen, especially those  $\mu\text{-SH}$  ligands in cationic dinuclear complexes because they are more acidic than those in corresponding neutral complexes. (Scheme 12)



Scheme 12 Proton transfer from metal-SH complexes to coordinated dinitrogen

Some transition metal clusters have been synthesized, which are analogues to the cubane subunit of the clusters in nitrogenases and hydrogenases, such as  $(\text{Et}_4\text{N})_2[(\text{Cl}_4\text{-cat})(\text{CH}_3\text{CN})\text{MoFe}_3\text{S}_4\text{Cl}_3]$ <sup>39</sup> ( $\text{Cl}_4\text{-cat}$  = tetrachlorocatecholate), (Figure 5 a) and  $[\text{Ru}_4\text{S}_4\text{Cp}^*_4]^{2+}$ <sup>40</sup> (Figure 5 b). It has been proved that  $[\text{Fe}_4\text{S}_4(\text{SR})_4]^{2-}$  ( $\text{R} = \text{Ph}, \text{C}_6\text{H}_4\text{Me}$ ) can catalyze the reduction of diphenylacetylene to cis-stilbene by excess sodium borohydride in  $\text{CH}_3\text{CN} / \text{MeOH}$ <sup>41</sup>. The  $(\text{Et}_4\text{N})_2[(\text{Cl}_4\text{-cat})(\text{CH}_3\text{CN})\text{MoFe}_3\text{S}_4\text{Cl}_3]$  cluster, in which Mo atom has a coordination environment very similar to that in nitrogenases, can catalyze the four-electron reduction of  $\text{N}=\text{N}$  bond of cis-dimethyldiazene giving methylamine.

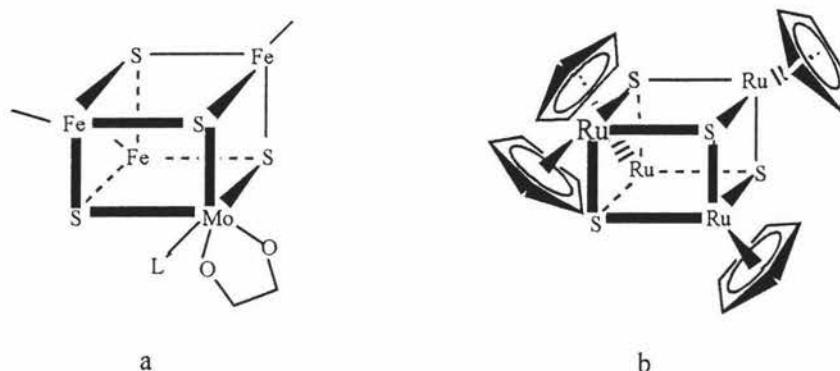


Figure 5 Structures of  $(\text{Et}_4\text{N})_2[(\text{Cl}_4\text{-cat})(\text{CH}_3\text{CN})\text{MoFe}_3\text{S}_4\text{Cl}_3]$  and  $[\text{Ru}_4\text{S}_4\text{Cp}^*_4]^{2+}$

Many ruthenium sulfur clusters have been synthesized and characterized. Most of them are CO containing clusters such as  $[\text{Ru}_6\text{S}_3(\text{H})(\text{CO})_{15}]^{42}$ . A Ru-Mo cluster  $[\{\text{CpMo}(\text{CO})_2\}_2\text{SRu}(\text{CO})_3]$  that contains a  $\mu_3$ -sulfide ligand, which has the same mode of coordination as in  $[(p\text{-cymene})_3\text{Ru}_3\text{S}_2]^{2+}$ , was found to promote a nonreductive coupling of alkynes <sup>43</sup>.

## 1.2. Transition metal sulfur complexes for catalysis --- hydrodesulfurization (HDS)

Transition metal complexes are widely used for catalysts. Hydrodesulfurization is one of their very important applications.

The hydroprocessing of petroleum represents one of largest scale chemical processes carried out by industries in the world today. In this procedure, crude oil is treated with hydrogen at high pressure (1500-3000 lbf in<sup>-2</sup>) over a hot heterogeneous catalyst (Co- or Ni- promoted, Mo or W sulfide supported on  $\text{Al}_2\text{O}_3$ ) (500 – 825°C) to

remove nitrogen, sulfur and residue metals prior to further processing<sup>44</sup>. The removal of sulfur from residues in oil is commonly referred to as hydrodesulfurization.

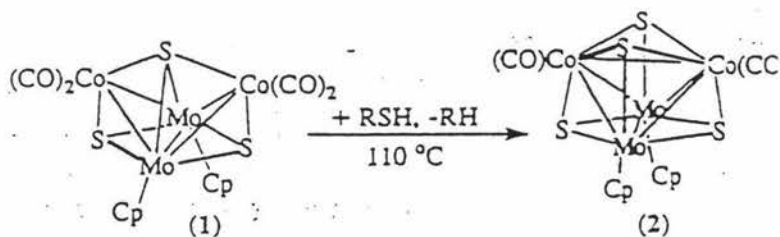
On one hand, since new drilling techniques allow the recovery of heavier crude oils that contain higher levels of sulfur, removal of this element is becoming even more important, particularly for those countries that possess very large reserves of heavy crudes. On the other hand, recent environmental pollution regulations require lower amounts of sulfur in fuels, which can not be achieved using known technology. Thus there is increasing interest in developing new catalysts and processes for the removal of sulfur from the organosulfur compounds in petroleum.

### 1.2.1 Industry catalysts and mechanisms

Many metals are more active as HDS promoters than cobalt or nickel mixture. The active sequence has been proven to be:  $\text{Ni} < \text{Co} < \text{Pd} < \text{Pt} < \text{Re} < \text{Ir} < \text{Rh} < \text{Os} \leq \text{Ru}$ <sup>45</sup>. That is, ruthenium is the most active promoter compared to other metals in HDS processes while cobalt and nickel are still the metals of choice for current industry use. A good heterogeneous catalyst of Co/Mo/S compositions and the related Ni/W/S systems are widely used to catalyze the HDS of fossil fuel feedstocks<sup>46</sup>. The catalyst is conventionally prepared by impregnating a high-sulfur-area alumina with ammonium molybdate and a cobalt salt in an aqueous medium. This pre-catalyst is then treated with hydrogen and a source of sulfur ( $\text{H}_2\text{S}$ , organic sulfur compounds, or the feedstocks) at temperature near  $350^\circ\text{C}$ . This sulfidation step converts the molybdenum oxides into a  $\text{MoS}_2$ -like phase that gives metal-sulfur cores indicating the active sites<sup>47</sup>.

Under the reducing atmosphere of high  $\text{H}_2$  pressures, the surfaces of these sulfides exhibit coordinatively unsaturated reduced metal sites. A redox HDS mechanism involves binding of thiophene at one of these electron rich sites, oxidative addition, sulfur removal and reduction of the metal<sup>48</sup>. A recently study on soluble transition metal sulfur clusters in homogeneous catalytic systems has proved this. A cluster  $[(\text{Cp}')_2\text{Mo}_2\text{Co}_2\text{S}_3(\text{CO})_4]$  ( $\text{Cp}'$

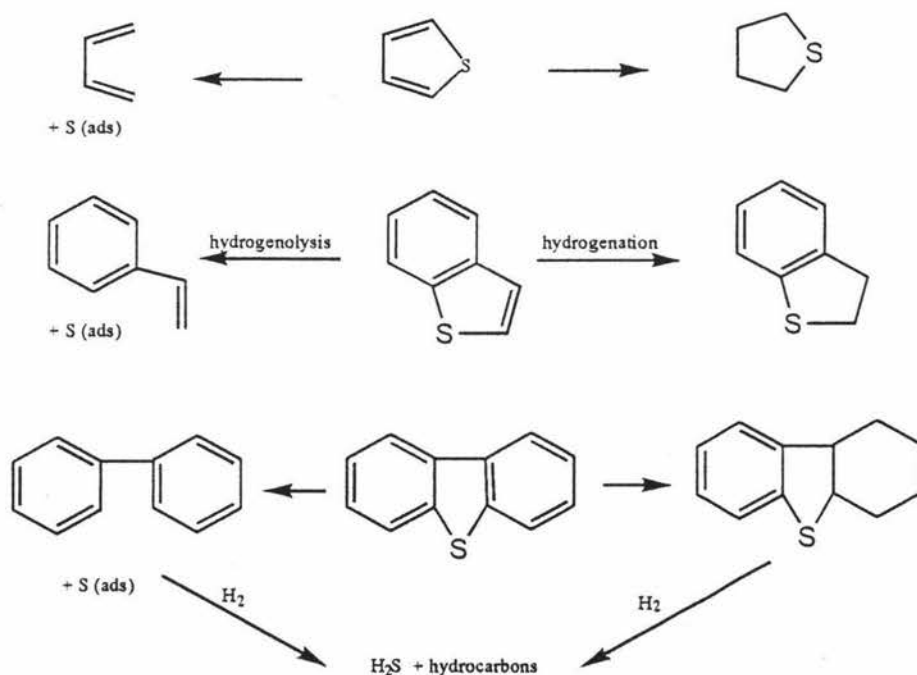
=  $\text{CH}_3\text{C}_5\text{H}_4$ ) with  $\mu_3$ - and  $\mu_4$ -sulfur ligands could remove sulfur directly from thiophene producing a cubane cluster  $[(\text{Cp}')_2\text{Mo}_2\text{Co}_2\text{S}_4(\text{CO})_2]$  (scheme 14)<sup>49, 47, 50</sup>.



Scheme 14 Sulfur atoms removed by  $[(\text{Cp}')_2\text{Mo}_2\text{Co}_2\text{S}_3(\text{CO})_4]$

The principal mechanism proposed for the heterogeneous HDS of thiophenes is summarized in Scheme 4<sup>51</sup>.

From the scheme, it can be seen that hydrogenation and hydrogenolysis are the main parts in the HDS process of thiophenes.

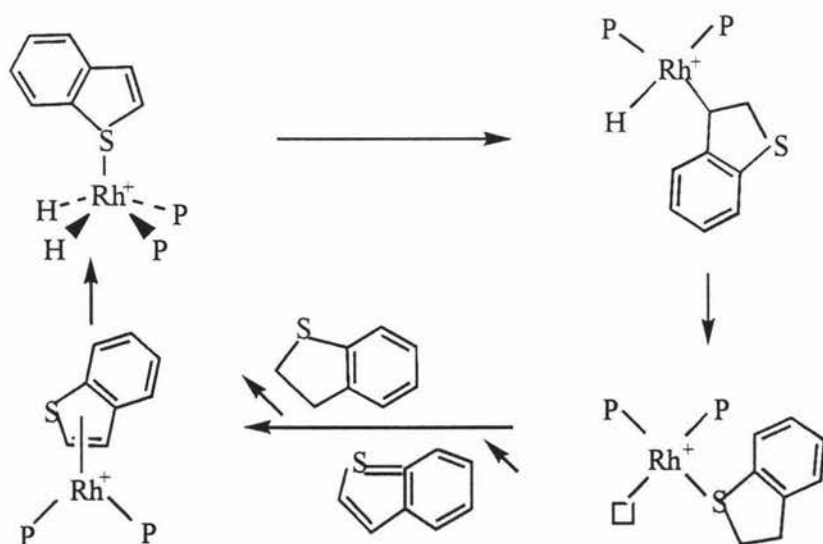


Scheme 4 The principal mechanism for heterogeneous HDS of thiophene

## 1.2.2 Catalytic hydrogenation reactions

The development of efficient catalysts for plain hydrogenation of thiophenes remains an important goal in HDS chemistry. In fact, the cyclic thioether products can subsequently be desulfurized over conventional HDS catalysts under milder reaction conditions than those necessary to accomplish the hydrodesulfurization of the thiophene precursors. This aspect is particularly important for the benzothiophenes and dibenzothiophenes because the conventional catalysts can desulfurize the corresponding cyclic thioethers, dihydrobenzothiophenes and hexahydrodibenzothiophenes, without affecting the benzene rings, necessary to preserve a high octane number.

Several homogeneous hydrogenation reactions of the model substrate benzothiophene to dihydrobenzothiophene have been carried out over the last fifteen years<sup>52, 53, 54, 55</sup>, such as  $[\text{RuCl}_2(\text{PPh}_3)_3]$ ,  $[\text{RuH}(\text{Cl})(\text{CO})(\text{PPh}_3)_3]$ <sup>56</sup> and  $[\text{Rh}(\text{Cp}^*)(\text{MeCN})_3][\text{BF}_4]_2$ , etc. The proposed mechanism of hydrogenation using  $[\text{Rh}(\text{cod})(\text{PPh}_3)_2]^+$  (cod = cycloocta-1,5-diene) is shown in Scheme 5<sup>54</sup>.



Scheme 5 The proposed mechanism of hydrogenation using  $[\text{Rh}(\text{cod})(\text{PPh}_3)_2]^+$

At comparable donor-atom sets of the catalytic precursor, the hydrogenation activity increases in the order of Ir < Rh < Ru ≤ Os, which is not far away from the trend observed for the heterogeneous HDS of dibenzothiophenes<sup>57</sup>. That is, ruthenium is almost the most active catalytic precursor in these processes.

### 1.2.3 Catalytic hydrogenolysis reactions

For hydrogenolysis reactions, those metal-mediated transformations of thiophenes that result in the opening and hydrogenation of the substrates to give the corresponding unsaturated thiols, which eventually are reduced to the saturated derivatives.

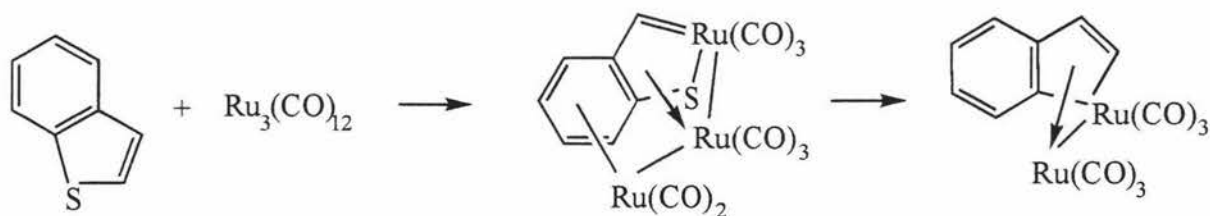
For the reasons put forward in the case of the hydrogenation, the hydrogenolysis reactions of thiophenes are of great relevance for the conventional heterogeneous catalysts under milder conditions than those required to desulfurize the thiophenes directly.

Ruthenium is also very active in these catalytic processes. A similar trend of activity is shown by the heterogeneous HDS catalysts, which emphasizes the great catalytic ability of ruthenium in these processes<sup>58</sup>.

### 1.2.4. Catalytic desulfurization reaction

Several transition metal cluster based systems have been developed evolving desulfurizing organic compounds. All the desulfurization action reported<sup>59,60,61,62,63,64</sup> involves the concomitant action of two metals, one of which opens or activates the thiophene, while the other one promotes the extrusion of the sulfur atom. The later step can occur either thermally or by treatment with H<sub>2</sub>. Soluble clusters such as [Ru<sub>3</sub>(CO)<sub>12</sub>]<sup>65</sup> and [IrH(η<sup>2</sup>-C,S-C<sub>12</sub>H<sub>8</sub>S)(triphos)] (triphos = MeC(CH<sub>2</sub>PPh<sub>2</sub>)<sub>3</sub>)<sup>66</sup> are capable of straight

forwardly desulfurizing thiophenes giving catalytic amount of biphenyl and  $\text{H}_2\text{S}$  under relatively mild condition. (Scheme 6)



Scheme 6 Desulfurization of thiophenes by  $[\text{Ru}_3(\text{CO})_{12}]$

### 1.3. Nitrogenases and dinitrogen reduction

While reduced dinitrogen is an integral component of proteins, nucleic acids and most other biomolecules, dinitrogen is regarded as one of the most inert molecules under laboratory condition because of the large activation energy required to form ammonia. Consequently, acquisition of metabolically usable forms of nitrogen is essential for the growth and survival of all organisms, which implies that dinitrogen reduction is one of the most basic energy sources of human beings. Although elemental dinitrogen is abundant in the earth's atmosphere, the great difficulty of reducing it to a usable form has been known for one century. The tough conditions of dinitrogen reduction in industries have already been shown earlier in Haber-Bosch process.

On the other hand, some bacteria containing nitrogenases can reduce atmospheric dinitrogen to ammonia under ambient condition.

There are three distinct kinds of nitrogenases, each of which consists essentially of two proteins. The most common nitrogenase contains iron and molybdenum but more recently two variants have been characterized. They are based upon iron and vanadium, and upon iron alone, respectively. The first one has been widely studied.



The molybdenum nitrogenase consists of two metalloproteins, the iron (Fe-) sulfur protein and the molybdenum iron (MoFe-) sulfur protein. The two clusters are P-cluster and Mo-cofactor, respectively, which are the active sites in the proteins. (Figure 6) Together, these proteins mediate the ATP-dependent reduction of dinitrogen to ammonia.

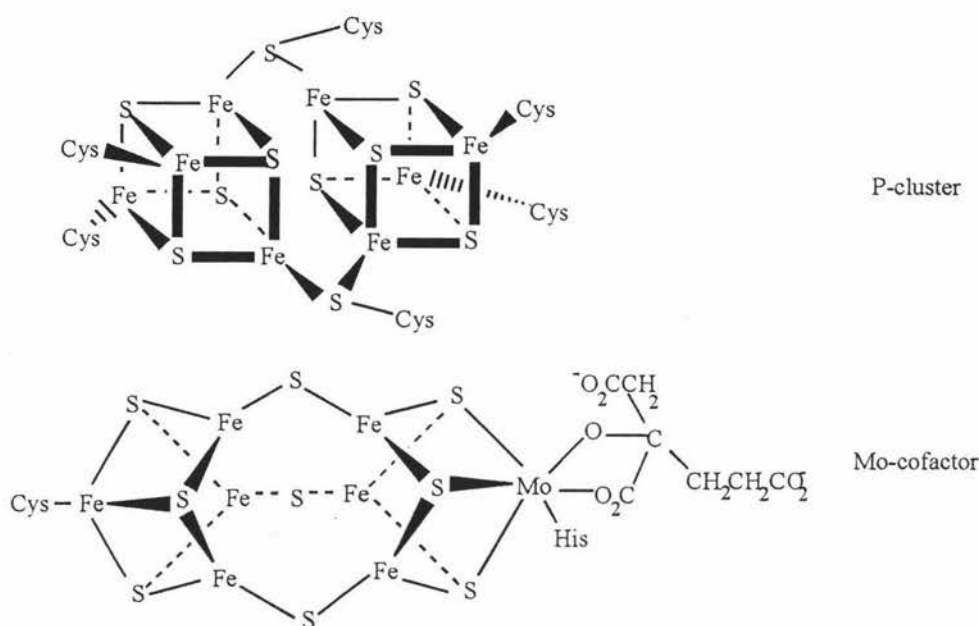
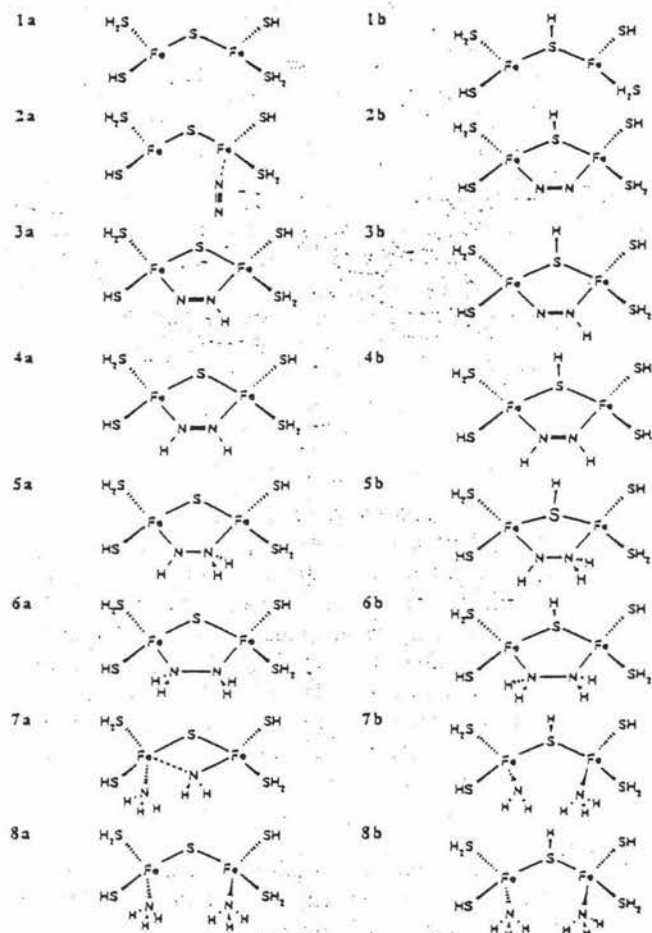


Figure 6 Structure of nitrogenase clusters

Currently, it has been discovered that the molybdenum atom is the dinitrogen binding site. Electrons are transferred from P-cluster to Mo-cofactor to achieve the dinitrogen reduction process.

It has been suggested that sulfur atoms in the clusters act in a key role of activating dinitrogen molecules in redox chemistry. A recent quantum chemical study on nitrogenases showed that the bridging sulfide ligands might be the main factor responsible for the activation of dinitrogen and for the subsequent formation of the N-H bonds. When a hydrogen atom binds onto the bridging sulfur, the way that dinitrogen bind onto the cluster might change from end-on coordination to one of the metal atoms to bridging

coordination between two metal atoms, which might increase the activity of dinitrogen to form ammonia<sup>3</sup> (scheme 7). For example, for the dimeric model, it is calculated that the addition of first hydrogen becomes exothermic by 55.9 kcal / mol for B (with hydrogen atom on the sulfur bridge) rather than 18.5 kcal / mol for A (without hydrogen atom on the sulfur bridge).



Scheme 7 Activation of dinitrogen by sulfur bridge with hydrogen on it

### 1.3.1 Transition metal mono- or bi-nuclear complexes in dinitrogen reduction

The existence of biological nitrogen fixation has inspired chemists to research for purely chemical systems capable of fixing dinitrogen catalytically under mild condition. Since 1960s, a lot of work has been done to mimic biological nitrogen fixation using transition metal complexes. Protonation of mono- or binuclear transition metal complexes with coordinating dinitrogens has been the most interesting area during the last three decades. It has been proven that many this kind of complexes can be protonated to give ammonia or other intermediate compounds such as hydrazine in lower temperature and pressure <sup>67</sup>.

There are mainly two ways that dinitrogen molecules coordinate to the metal atoms in mono- or bi-nuclear complexes: end-on coordination to one metal atom or bridging coordination between two metal atoms, which have been mainly studied. In  $[\text{RuH}_2(\text{N}_2)(\text{PPh}_3)_2]$  <sup>68</sup> and  $\text{cis-}[\text{Mo}(\text{N}_2)(\text{PMe}_2\text{Ph})_4]$  <sup>69</sup>, etc, the end-on coordinating dinitrogen can be reduced to ammonia at fairly mild conditions. In  $[\{\text{Zr}(\text{C}_5\text{Me}_5)_2(\text{N}_2)\}(\text{N}_2)]$  <sup>70</sup> and  $[\text{WCp}^*\text{Me}_2(\text{OC}_6\text{F}_5)]_2(\text{N}_2)$  <sup>71</sup> etc., dinitrogen coordinating between two metal atoms can be reduced indirectly.

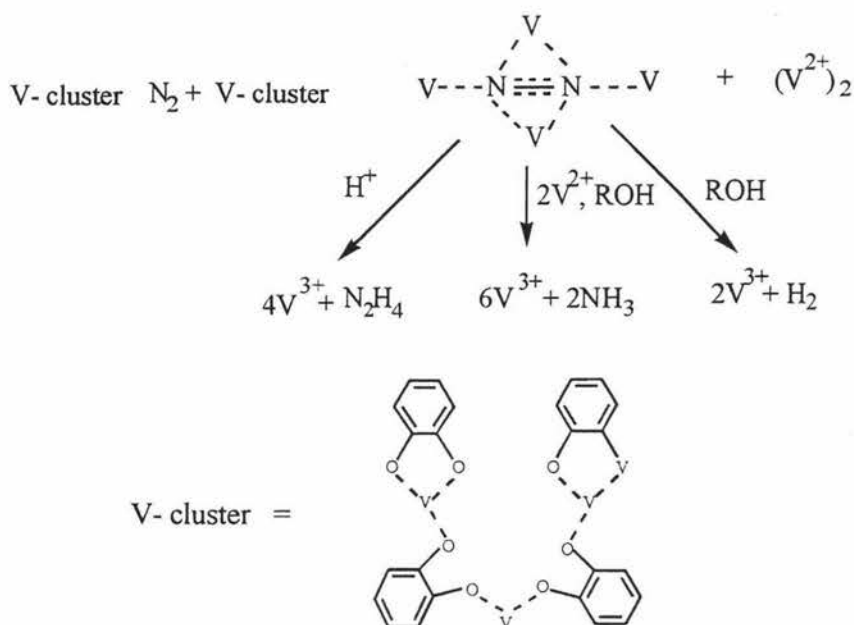
Recently Hidai et al. found the first bimetallic catalytic system that tungsten dinitrogen complex  $\text{cis-}[\text{W}(\text{N}_2)_2(\text{PMe}_2\text{Ph})_4]$  was treated with an equilibrium mixture of  $[\text{RuCl}(\text{dppp})_2]\text{X}$  and  $\text{trans-}[\text{RuCl}(\eta^2\text{-H}_2)(\text{dppp})_2]\text{X}$  ( $\text{X} = \text{BF}_4, \text{PF}_6, \text{or OSO}_2\text{CF}_3$ ;  $\text{dppp} = 1,3\text{-bis}(\text{diphenylphosphino})\text{propane}$ ) under 1 atmosphere of dihydrogen at 55 °C giving  $\text{NH}_3$  in moderate yield. It has been proven that the coordinating dinitrogen reacted with dihydrogen via the complexes with coordinating dihydrogen <sup>72</sup>.

### 1.3.2. Transition metal clusters in dinitrogen reduction

In dinitrogen reduction, the catalysts are expected to be poly-nuclear clusters with a maximum number of contacts with nitrogen during the catalysis process.

When electrons transfer to dinitrogen in a metal complex, bond formation must compensate for the energy of NN bond loosening. Apparently, the larger the number of metal atoms directly bound to dinitrogen, the easier it is to reach the same extent of NN bond weakening, since each metal provides electrons to NN bond and therefore, is already a reductant at the stage of complex formation. Therefore, it might be expected that a three- or even four-nuclear complex would activate dinitrogen more effectively than mono- or binuclear complexes. It is suggested that when dinitrogen bind on cluster  $[V_3(\text{catecholate})_3]$ , a tetranuclear intermediate might be formed (Scheme 8)<sup>73</sup>.

Besides the way that the dinitrogen binds on the metal atoms, the number of the electrons that the cluster can store and transfer to the dinitrogen molecule for the requiring of breaking the NN bond is also very important in catalytic process. It needs six electrons altogether to reduce the dinitrogen to ammonia, which is difficult to achieve for mono- or bi-nuclear complexes. Sometimes, clusters can open their structures by breaking one metal-metal bond during electron storing and transferring processes, which implies larger abilities of catalysis than mono- or binuclear complexes.



Scheme 8 Tetranuclear intermediate of dinitrogen binding on  $[\text{V}_3(\text{catcholate})_3]$

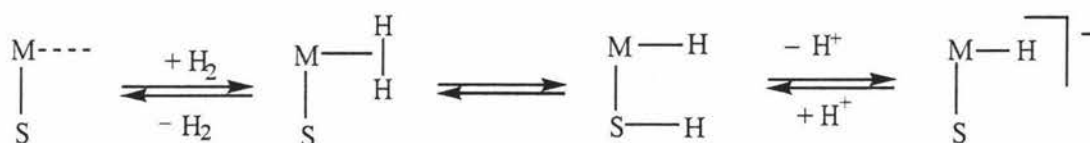
## 1.4. Clusters in hydrogenases and hydrogenation

The formation and consumption of dihydrogen by microorganisms are catalyzed by hydrogenases. Beside the hydrogenases without nickel and iron-sulfur clusters in *methanogenic archaea*<sup>74</sup>, the other two types of metal clusters in hydrogenases are  $[\text{Ni}, \text{Fe}, \text{S} \text{ or } \text{Se}]$  and  $[\text{Fe}, \text{S}]$ . Both of the clusters exhibit sulfur-rich coordination spheres, which are believed to be the dihydrogen activation sites<sup>75, 76</sup>. On the basis of redox titrations and EPR spectra, it has been suggested that the nickel atom and iron atom are the dihydrogen binding sites in  $[\text{NiFe}]$  hydrogenases and nickel-free “iron only” hydrogenases, respectively. Both enzymes catalyze the redox equilibrium and the heterolytic cleavage of dihydrogen (Scheme 9)<sup>77</sup>:



Scheme 9 Redox equilibrium catalyzed by hydrogenases

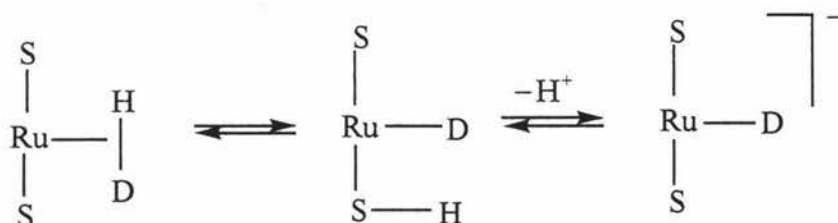
The proposed mechanism is shown in Scheme 10:



Scheme 10 The proposed mechanism of heterolytic cleavage of dihydrogen

The metal-sulfur sphere cleaves the dihydrogen via formation of  $\eta^2\text{-H}_2$  and thiol species.

Recently, Sellmann et.al found that the dihydrogen molecule can heterolytically be cleaved at ruthenium sulfur sites of cluster  $[\text{Ru}(\text{PCy}_3)(\text{'S}_4\text{'})]$  ( $\text{'S}_4\text{'}$  = 1,2-bis((2-mercaptophenyl)thiol)ethane(2-)) in the presence of NaOMe at very mild condition (Scheme 11) <sup>78</sup>.

Scheme 11 Dihydrogen cleaved at Ru-S sites of cluster  $[\text{Ru}(\text{PCy}_3)(\text{'S}_4\text{'})]$

In this case, thiol hydride species could not yet be detected. However, an experiment on analogue rhodium cluster has been proven<sup>79</sup>. They both yield model compounds that combine structural and functional feature of the active centers in hydrogenases.

## **1.5. New arene ruthenium sulfur clusters**

It has been shown that transition metal sulfur compounds play very important roles in a range of biological and industrial processes.

The potential for insights into these processes from sulfur containing clusters is large. The next chapter of this thesis explores the synthesis and characterization of the new high nuclearity arene-ruthenium-sulfur clusters